ACS Photonics

Review

Cite This: ACS Photonics XXXX, XXX, XXX-XXX

pubs.acs.org/journal/apchd5

Controlling the Optical Response of 2D Matter in Standing Waves

Eric Plum,[*,†] Kevin F. MacDonald,[*,†] Xu Fang,[‡] Daniele Faccio,[§] and Nikolay I. Zheludev[*,†,∥]

[†]Optoelectronics Research Centre and Centre for Photonic Metamaterials and [‡]Department of Electronics and Computer Science, University of Southampton, Highfield, Southampton, SO17 1BJ, United Kingdom

[§]School of Engineering and Physical Sciences, SUPA, Heriot-Watt University, Edinburgh EH14 4AS, United Kingdom

[∥]Centre for Disruptive Photonic Technologies, School of Physical and Mathematical Sciences and The Photonics Institute, Nanyang Technological University, Singapore 637371

ABSTRACT: There is a major development unfolding in photonic technology that promises to impact optical data processing, spectroscopy, and nonlinear/quantum optics. This new direction relates to plasmonics, metamaterials and coherent optics. It exploits the difference in manifestations of optical properties of thin films in traveling waves and standing waves. In standing waves, "coherent control" of the energy exchange between incident and scattered waves leads to new technological opportunities including single photon gates, 100 THz all-optical modulators, sophisticated spectroscopy techniques that can for example distinguish different multipole contributions to absorption and quantum optical devices. We provide an overview of the rapidly growing body of work on the optics of films and metasurfaces in coherent light fields.

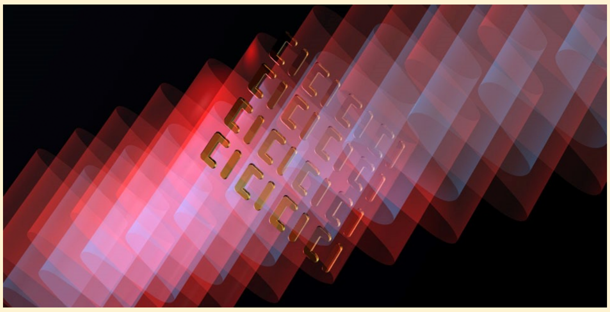

KEYWORDS: *standing wave, metamaterial, metasurface, plasmonics, all-optical, coherent perfect absorption*

Coherent control is a well-understood concept in quantum mechanics,[1] where it is used to direct dynamic processes with light by engaging quantum interference phenomena. Coherent control has also been employed to manipulate electron motion in semiconductors,[2] breaking of chemical bonds,[3] the absorption[4−8] and localization[9−13] of light in cavities and at surfaces, transmission of light by metal-dielectric stacks,[14,15] light modulation in waveguides,[16−18] nonlinear optical phenomena in periodic structures[19] and nanoparticles,[20] polarization rotation in Faraday media,[21,22] optical effects in optomechanical systems,[23,24] and the excitation and propagation of surface plasmon polaritons at metal/dielectric interfaces,[25−27] as well as the absorption of acoustic waves,[28,29] see Figure 1.

Here we review how coherent control of standing waves can be used to manipulate all kinds of light-matter interactions in thin films where one can change reflection, transmission, absorption and polarization properties. We begin with a theoretical description of such interactions followed by a review of the resulting opportunities from all-optical modulation of intensity, propagation direction, and polarization of light to their applications in data and image processing as well as quantum technologies.

Interaction of Coherent Light with 2D Matter. Consider a layer of absorbing material illuminated at normal incidence by a pair of counter-propagating, collinearly polarized coherent light waves: The incident fields E_α and E_β represent input signals; the transmitted and reflected waves (fields E_γ and E_δ) propagating away from the film on either side constitute output signals (Figure 2). Assuming a purely linear, isotropic dipolar response of the film, with no change in the polarization state of light, the input and output fields are related by a complex scattering matrix[30] $\mathbf{S}$:

$$\begin{bmatrix} E_\delta \\ E_\gamma \end{bmatrix} = \begin{bmatrix} \mathbf{S}_{11} & \mathbf{S}_{12} \\ \mathbf{S}_{21} & \mathbf{S}_{22} \end{bmatrix} \begin{bmatrix} E_\alpha \\ E_\beta \end{bmatrix} \quad (1)$$

where $\mathbf{S}_{11}$ and $\mathbf{S}_{21}$ are, respectively, the reflection and transmission coefficients for light incident on the medium from side 1; $\mathbf{S}_{22}$ and $\mathbf{S}_{12}$ being the same for incidence on side 2. In the absence of any magneto-optical effects, reciprocity dictates that $\mathbf{S}_{12} = \mathbf{S}_{21}$, so three independent parameters are necessary to describe the optical properties of such a device.

In this four-port optical device linearity of the film's properties implies that if both input signals are scaled by the same factor η, both of the resulting output signals must also scale by η. However, linearity of the film's response does not imply any proportional scaling of one, other, or both outputs when only one of the inputs is changed. In fact, the relationship between a given input port and a given output port in a coherent four-port device can be nonlinear. This nonlinear response results from the coherent redistribution of energy between the ports.

Planar metamaterials or metasurfaces—man-made media structured on the subwavelength scale—provide unprecedented

Special Issue: 2D Materials for Nanophotonics

Received: August 15, 2017

DOI: 10.1021/acsphotonics.7b00921
ACS Photonics XXXX, XXX, XXX−XXX

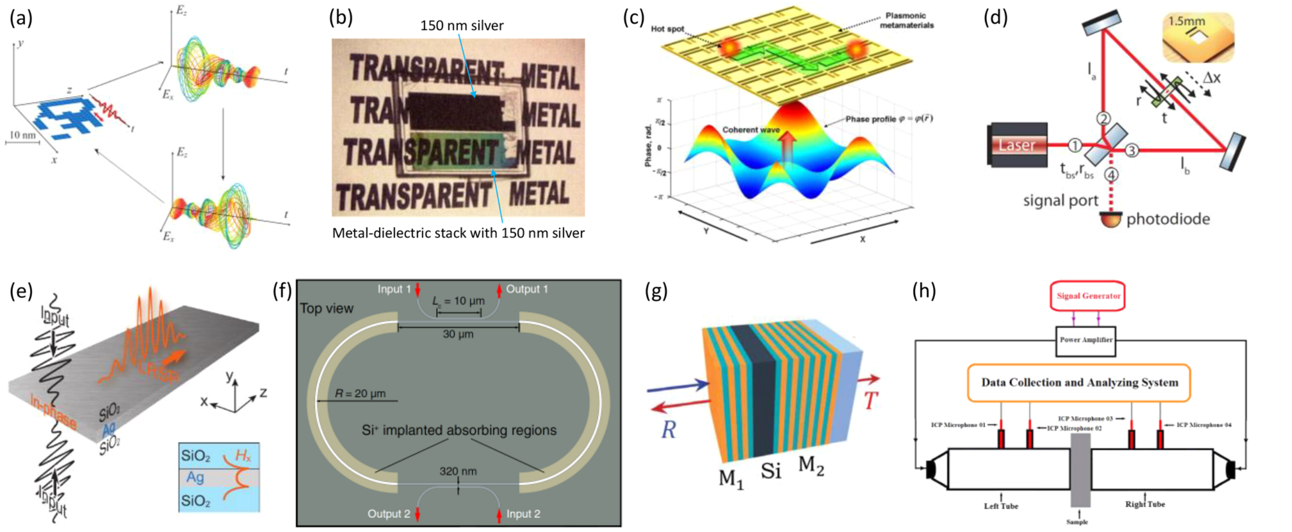

Figure 1. Coherent control of various phenomana across many disciplines. (a) Nanosecond-femtosecond spatiotemporal field localization in plasmonic systems by time reversal.[10] (b) Transparent metal-dielectric stacks.[15] (c) Nanoscale light localization in metamaterials.[11] (d) Quantum opto-mechanics based on destructive interference on a nanomembrane oscillator.[23] (e) Selective excitation of long-range surface plasmon polaritons.[27] (f) Silicon photonic modulator based on coherent perfect absorption.[18] (g) Multiband coherent perfect absorption in silicon controlled by aperiodic dielectric mirrors M.[8] (h) Coherent perfect absorption of sound.[29]

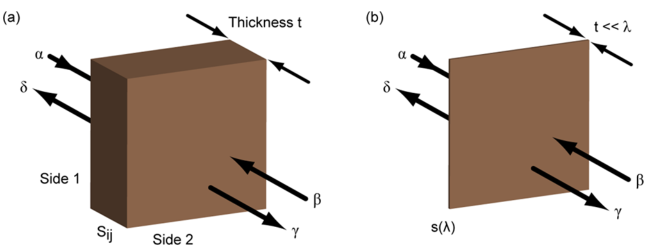

Figure 2. Generic four-port coherent control device. (a) A medium, with optical properties described by a complex scattering matrix $\mathbf{S}_{ij}$ containing three independent parameters, is illuminated by counter-propagating coherent input light waves α and β; waves γ and δ are the device outputs. (b) In the limit of substantially subwavelength thickness, the medium can be described by a single complex scattering coefficient $s(\lambda)$.

freedom to engineer the balance among resonant absorption, reflection and transmission almost at will in ultrathin metal, dielectric and semiconductor films. Nanostructuring of thin-film materials introduces optical resonances with a strength and spectral position that is controlled by the geometry and size of the nanostructure, allowing strong light−matter interactions to be achieved in films of nanoscale thickness and enabling the four-port optical device to be configured to deliver a broad range of functionalities.

Consider now a film of sufficient thinness that retardation effects across it can be ignored, that is, we may consider each constituent molecule to be exposed to the same electric field, the combined field $E_\alpha + E_\beta$ of the incident waves. Here energy will be reradiated equally in the forward and backward directions with an efficiency dependent on the excitation wavelength λ, resulting in a reradiated field $s(\lambda)(E_\alpha + E_\beta)$, where $s(\lambda)$ is the complex wavelength-dependent scattering coefficient for the film as measured in a traveling wave.[31] The magnitude and phase of $s(\lambda)$ respectively correspond to the relative amplitude of the reradiated field and to the phase lag between reradiated and driving fields. $s(\lambda)$ may include losses and thereby excludes any assumption of equality between the combined incident and combined output beam intensities. Requirements of field continuity then dictate the following scattering matrix expression relating input and output fields for a coherent four-port device based upon a vanishingly thin film (Figure 2b):

$$\begin{bmatrix} E_\delta \\ E_\gamma \end{bmatrix} = \begin{bmatrix} s(\lambda) & s(\lambda)+1 \\ s(\lambda)+1 & s(\lambda) \end{bmatrix} \begin{bmatrix} E_\alpha \\ E_\beta \end{bmatrix} \tag{2}$$

In cases where the contribution from interference among multiply reflected/transmitted beams is small, eq 2 can serve as an approximation to eq 1 for films of substantially subwavelength thickness and greatly simplifies the analysis of four-port coherent device functionalities by reducing the number of free parameters required to describe the system from three ($\mathbf{S}_{ij}$) to one, in the form of $s(\lambda)$.

At the node of a standing wave formed by counter-propagating coherent incident beams, $E_\alpha = -E_\beta$. With an ultrathin medium positioned at the node, E_γ will thus always be equal to E_α, and E_δ to E_β, regardless to the value of the film's scattering parameter $s(\lambda)$. This is the "coherent perfect transmission" regime, a situation in which there is no light−matter interaction because the film is located at a point where the electric field is zero. (It should be noted here that the regime of coherent perfect transparency of weakly absorbing films has long been exploited for intra-cavity laser mode selection.[32−37]) At an antinode of the standing wave, on the other hand, $E_\alpha = E_\beta$. Here, both E_γ and E_δ can be reduced to zero if $s(\lambda) = -0.5$, whereby the film exhibits the maximum possible level of zero-thickness single-beam absorption[38,39] of 50%. This is the regime of "coherent perfect absorption". It is interesting to note here that while perfect transparency requires an absorber of substantially subwavelength thickness,[40] the phenomenon of coherent perfect absorption does not. Indeed, the latter has been demonstrated in a variety of optically thick media and spectral domains.[5,8,41−43]

The effective optical nonlinearity of coherent four-port devices, that is, the nonlinear relationship between selected

DOI: 10.1021/acsphotonics.7b00921
ACS Photonics XXXX, XXX, XXX−XXX

input and output port intensities, is illustrated by the intensity (defined as $I = EE^*$) of output γ:

$$I_\gamma = |1 + s(\lambda)|^2 I_\alpha + |s(\lambda)|^2 I_\beta + 2Re\{(1 + s(\lambda))s^*(\lambda)E_\alpha E_\beta^*\} \quad (3)$$

Clearly, if one of the two input signals is removed, the output signal intensities are strictly proportional to that of the remaining input. And, if input intensities I_α and I_β are increased or decreased in proportion, there will be a correspondingly proportional increase or decrease in I_γ. However, if I_α remains fixed and only I_β changes, then I_γ will respond in a nonlinear fashion, as illustrated in Figure 3 for the case where $s(\lambda) = -0.5$ and $I_\alpha = 1$: here the dependence of I_γ on I_β is nonlinear.

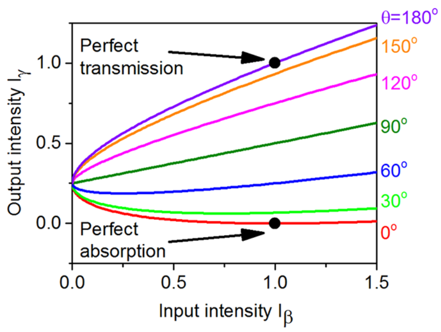

Figure 3. Nonlinear response function of a generic four-port coherent device. Dependence of output intensity I_γ on input intensity I_β for a fixed input intensity $I_\alpha = 1$, for a selection of mutual phase settings θ between E_α and E_β (as labeled) in the plane of a vanishingly thin absorber with a scattering parameter $s(\lambda) = -0.5$.

Light propagating in a conventional nonlinear (bulk) medium experiences harmonic distortion, which can lead ultimately to optical instability and multistability. The nonlinear character of a four-port coherent device, however, is different: it is based on the redistribution of energy among ports and does not cause harmonic distortion; it is underpinned only by linear interference effects and as such is of course strictly compliant with energy conservation; a variety of functionalities is enabled by the fact that the level of absorption in such devices is strongly dependent on the balance of intensities and mutual phase of the input beams.

It is apparent from the above analysis that an effective nonlinearity may be obtained using any ultrathin film, for example, a 50:50 beamsplitter. However, in dissipation-free films the range of achievable input-output functions is constrained. In this context, photonic metamaterials provide access to an otherwise inaccessible range of ultrathin-film scattering coefficients $s(\lambda)$ at any desired wavelength by nanostructural design, and thereby to a wide range of nonlinear response functions.

Before illustrating specific metamaterial designs and four-port device functionalities based upon such structures, we shall consider the meaning of $s(\lambda)$ scattering coefficients. For instance, single-pass absorption is governed by the expression

$$A = 1 - |s(\lambda)|^2 - |s(\lambda) + 1|^2 \quad (4)$$

Figure 4a maps levels of single-beam absorption onto the complex $s(\lambda)$ parameter space. The red circular line corresponds to $A = 0$ and describes lossless media that neither absorb nor amplify incident light. It defines a boundary between absorbing materials ($A > 0$, inside the circle) and gain media ($A < 0$, outside the circle). The central point of the circle $A = 0.5$ represents the maximum possible level of single-beam absorption permitted by field continuity constraints in a vanishingly thin film.[38,39] It corresponds to a film with a scattering parameter $s(\lambda) = -0.5$.

A perfectly transparent thin film that does not inflict any phase change corresponds to $s(\lambda) = 0$. A thin film of perfect electric conductor (PEC), on the other hand, will reflect 100% of incident light at any wavelength with a π phase change corresponding to $s(\lambda) = -1$. Scattering coefficients for glass films with a refractive index of 1.5 also sit on the zero-loss contour, being represented over a given wavelength range by a segment of a circle, as opposed to a singular point, as plotted in Figure 4b for glass films of 10 and 50 nm thicknesses for wavelengths from 750 to 1050 nm. Gold thin films are dispersive but highly reflective and weakly absorbing, so they appear in $s(\lambda)$ space as curves lying just inside the zero-loss contour.

In contrast, metamaterial nanostructures can provide access by design to the full parameter space. This is illustrated by Figure 4c, showing the range of scatting coefficients accessible with several planar metamaterial designs of sub-100 nm

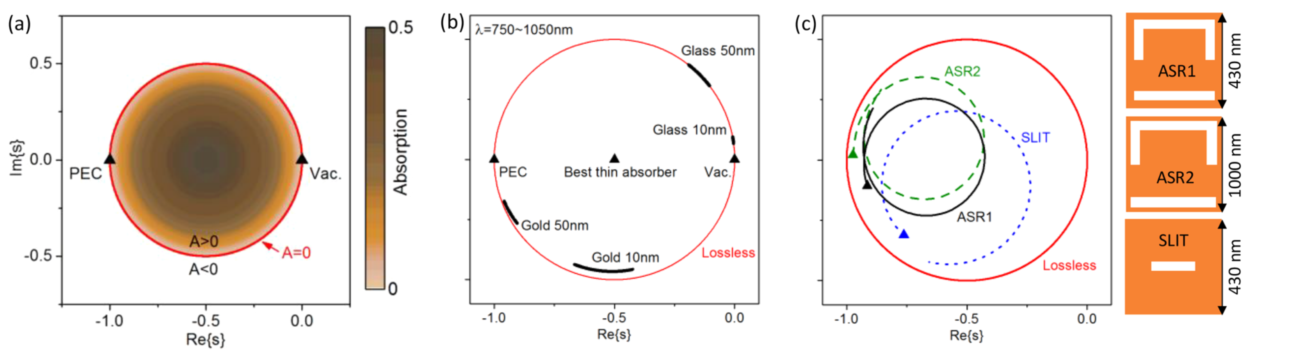

Figure 4. Scattering coefficient $s(\lambda)$ of ultrathin films and associated properties. (a) Level of absorption A of an ultrathin film illuminated from only one side as a function of its scattering coefficinet s. (b) Scattering coefficients for homogeneous thin film media in the 750−1050 nm wavelength range. (c) Scattering coefficients for selected periodic planar metamaterials indicated by their unit cells, modeled in COMSOL Multiphysics. The designs ASR1, ASR2, and SLIT consist of gold on silicon nitride with layer thicknesses of 50/30, 50/30, and 30/30 nm and the scattering coefficients are plotted for wavelength ranges of 750−1050, 1250−1850, and 750−1050 nm, respectively, with a triangular marker indicating the shortest wavelength. Modeling assumed a Drude-Lorentz model for the properties of gold and a fixed refractive index of 2.0 for silicon nitride, with normal monochromatic plane-wave illumination linearly polarized with the electric field parallel to the common symmetry axis of the nanostructures.

DOI: 10.1021/acsphotonics.7b00921
ACS Photonics XXXX, XXX, XXX−XXX

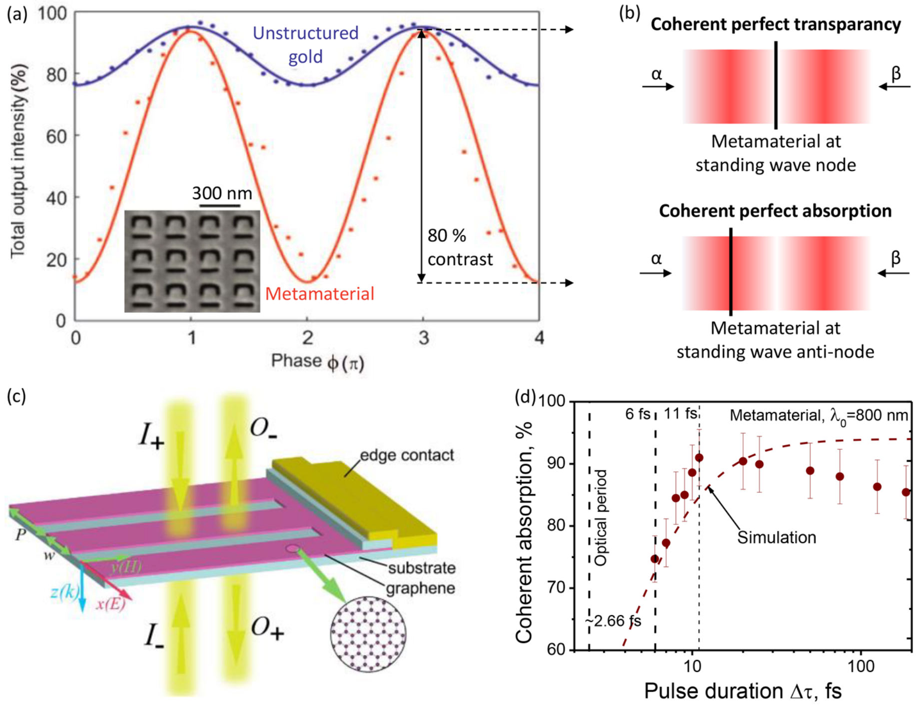

Figure 5. Coherent absorption modulation in 2D matter. (a) First observation of coherent absorption and transparency for a planar metamaterial (50 nm thick nanostructured gold supported by glass) illuminated by counterpropagating coherent laser beams at 633 nm wavelength linearly polarized parallel to the symmetry axis of the nanostructure.[40] (b) Schematic illustrating coherent perfect transparency and absorption resulting from destructive and constructive interference of incident electric fields α and β on a planar metamaterial. (c) Proposed scheme for electric control of mid-infrared coherent absorption in structured graphene.[50] (d) Coherent absorption at the standing wave antinode measured with counterpropagating coherent femtosecond laser pulses for a plasmonic metamaterial consisting of a freestanding 60 nm thick gold film perforated with an ASR aperture array of 320 nm period.[47]

thickness. These are arrays of asymmetric split ring (ASR) and slot apertures in a bilayer of gold and silicon nitride. ASR designs have been employed and optimized in numerous previous studies,[44,45] including the first experimental demonstrations of coherent absorption modulation.[40,46] The scattering coefficients of metamaterial ASR1 for wavelengths between 750 and 1050 nm describe a loop extending from the neighborhood of the zero-loss contour, toward the center of the $A > 0$ domain with "ideal, zero-thickness absorber" characteristics at 870 nm wavelength, and back. The metamaterial response can be modified simply by adjusting the dimensions of the design: the ASR2 line for example represents a similar pattern with an absorption resonance centered at 1550 nm. The third trace presented in Figure 4c corresponds to a metamaterial comprising an array of linear slots in a gold film on silicon nitride. Thus, metamaterials can provide otherwise unattainable thin film optical properties by nanostructural design.

Coherent Modulation of Absorption. As explained above, the interference of coherent light beams on an ultrathin layer of material, much thinner than the wavelength of light, can selectively render the medium almost perfectly transparent or facilitate near-perfect optical absorption, thus enabling high bandwidth light-by-light modulation[47] at low intensity.[48]

As noted earlier, coherent control of absorption in standing waves has long been exploited for laser mode selection, whereby a lossy thin film is placed within the laser cavity at a node of the desired mode to selectively absorb competing modes.[32−37] Coherent perfect absorption in thick structures,[8,41] − sometimes referred to as time-reversed lasing,[4,5,42,43] has also been known for some time.

Dynamic coherent control of thin film absorption from coherent perfect transparency to coherent perfect absorption was first observed by Zhang et al.[40] for a 50 nm thick gold film perforated with an ASR aperture array and supported by a glass substrate using a HeNe laser (Figure 5a). In the absorber, that was 13× thinner than the laser wavelength, a full span of modulation from nearly perfect absorption to nearly perfect transmission was demonstrated. When the absorber is placed at an electric field node of the standing wave no light-matter interaction occurs (Figure 5b). In contrast, if the metasurface is located at an antinode of the standing wave, the light−matter interaction is enhanced, resulting in nearly complete absorption of all incident light. Apart from photonic metasurfaces made from plasmonic materials,[40] dielectrics,[49] or graphene,[50] coherent perfect absorption and transparency has also been investigated in multiband microwave metamaterials[51] and heavily doped silicon thin films for terahertz waves[52] as well as observed in 9 nm thick (30-layer) graphene,[53] which exhibits broadband 50% absorption when illuminated by a single beam of light. Notably, the electric tunability of layered or structured graphene absorbers offers the interesting opportunity of electric modulation of coherent absorption,[50] see Figure 5c.

While optical nonlinearities suffer from a trade-off between speed and magnitude,[54] Xu, Nalla, and coauthors[46,47] have demonstrated that coherent absorption offers intensity-independent high contrast modulation of light-with-light even at femtosecond time scales which can be used for generation of "dark pulses". Figure 5d shows coherent absorption measured in a plasmonic metasurface with femtosecond laser pulses. Absorption of about 90% can be achieved with laser pulses as

DOI: 10.1021/acsphotonics.7b00921
ACS Photonics XXXX, XXX, XXX−XXX

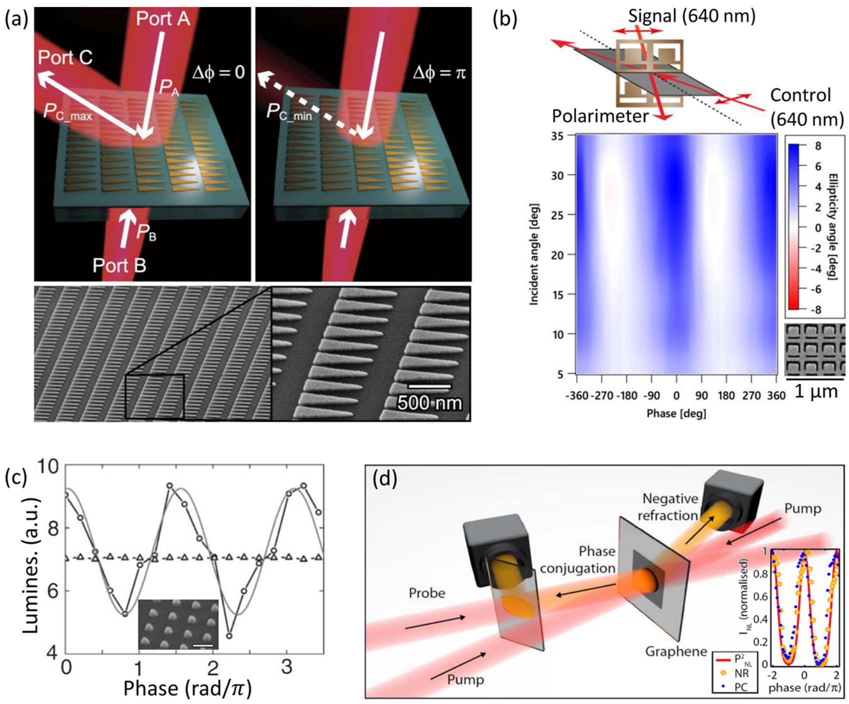

Figure 6. Coherent control of diffraction, polarization effects, and nonlinear phenomena in the optical part of the spectrum. (a) Constructive interference (left) of incident waves A and B on a phase-gradient metasurface leads to efficient redirection of light to Port C, while the diffracted beam vanishes almost completely in case of destructive interference (right).[57] (b) Manifestation of optical activity of a metasurface controlled by constructive interference (phase 0) and destructive interference (phase ± 180°) of 640 nm wavelength signal and control beams illuminating the nanostructure.[65] (c) Photoluminescence of dye molecules on aluminum nanopyramids (300 nm scale bar) as a function of the phase difference between coherent (circles) and incoherent (triangles) counterpropagating pump beams.[66] (d) Nonlinear response of 30-layer graphene controlled by constructive (phase 0) and destructive (phase π) interference of counterpropagating coherent pump beams on the nonlinear thin film at 780 nm wavelength. Time-averaged nonlinear polarization P^2_{NL}, as well as negatively refracted (NR) and phase-conjugated (PC) beam amplitudes, are shown.[67]

short as 10 fs, corresponding to about four optical cycles and a bandwidth on the order of 100 THz.

The ability to control absorption of light-with-light without a nonlinear medium, with 100 THz bandwidth and without need for high intensities opens up a broad range of possibilities. As discussed later on, the resulting effective nonlinearity may be used to achieve various logical functions for ultrafast all-optical data processing, image recognition and analysis, as well as small-signal amplification and coherence filtering.

Coherent Control of Diffraction, Polarization Effects, and Nonlinear Optical Phenomena. While the ability to control absorption is very important, coherent interaction of light-with-light on planar materials can go much further. The superposition of coherent waves allows control over both the local electric and the local magnetic field from zero (destructive interference) to enhancement (constructive interference). By controlling the field in the plane of a 2D material, the interaction of coherent light fields may therefore be used to control the optical excitation of the material and thus the manifestation of any optical functionality the material may have. Opportunities include control over diffraction from gratings or phase-gradient metasurfaces, the manifestation of linear and circular birefringence and dichroism, and the efficiency of nonlinear optical responses, promising new functionalities for wavefront shaping and signal processing.

For example, Shi et al.[55] studied coherent control of phase-gradient metasurfaces, which are planar metamaterials consisting of "meta-molecules" that scatter light with a spatially varying phase, resulting in diffraction, transmission and reflection of light.[56] Exploiting destructive interference of coherent light fields incident on the metasurface from opposite sides, scattering and thus diffraction may be turned off, whereas constructive interference yields diffraction with enhanced efficiency, enabling dynamic redirection of light. An experimental realization was recently reported by Kita et al.[57] using a gold phase-gradient nanostructure with a partial back reflector that directs scattered light preferentially to one side of the nanostructure, see Figure 6a. Such all-optical beam deflection could have applications in signal routing and the concept could be extended to planar meta-lenses[58,59] and meta-holograms,[60,61] that could also be coherently controlled.

Coherent control of polarization phenomena with very high contrast has been reported at microwave frequencies using anisotropic as well as 3D-chiral structures that are thin compared to the wavelength.[62] Coherent interaction of microwaves on an anisotropic metamaterial, resembling a wave plate, has allowed full control over the orientation of the plane of polarization. Arbitrary levels of polarization rotation have also been achieved with a chiral thin film consisting of mutually twisted metal patterns in parallel planes spaced by a distance of a small fraction of a wavelength. Optical activity—an ability to rotate the polarization state of light (circular birefringence), and differential throughput for left- and right-handed circular polarizations (circular dichroism)—is usually observed in such 3D-chiral structures (that is, in structures that cannot be superimposed with their mirror image). While 3D-chiral structures can be very thin, they cannot be planar, however optical activity does not require chiral materials.

DOI: 10.1021/acsphotonics.7b00921
ACS Photonics XXXX, XXX, XXX−XXX

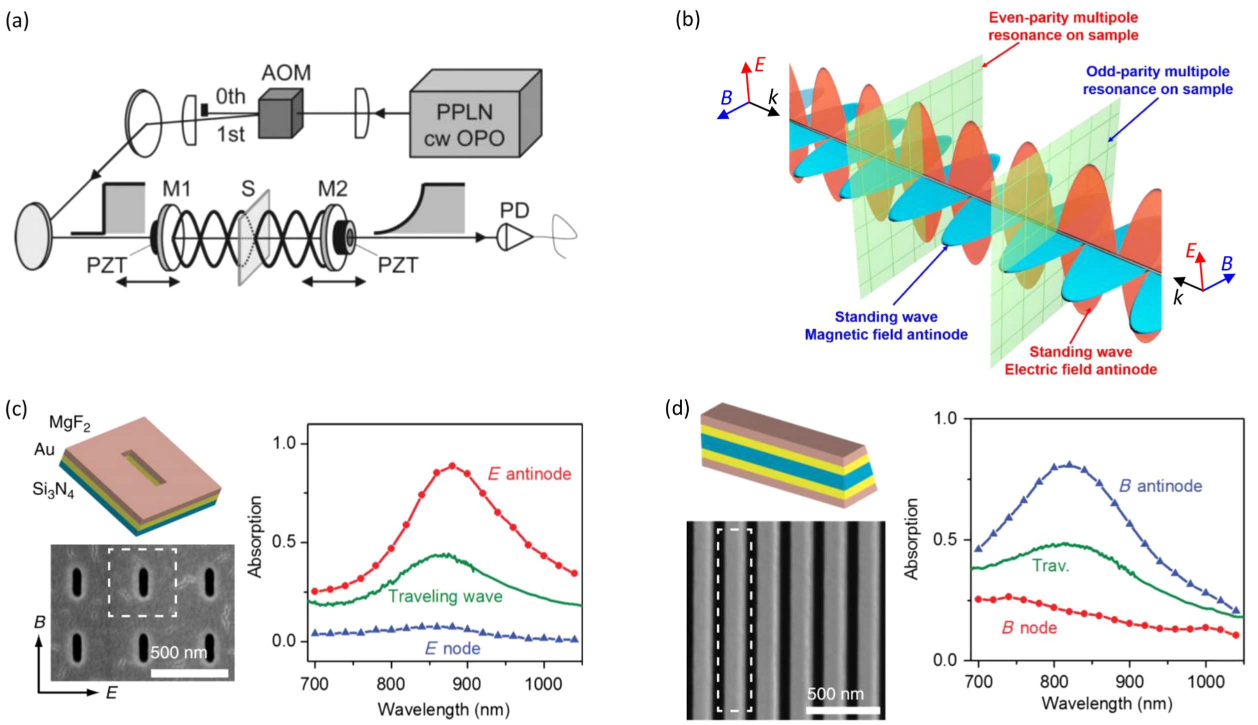

Figure 7. Coherent spectroscopy in standing waves. (a) Schematic setup for photon-trap spectroscopy, a generalized form of cavity ringdown spectroscopy where a thin sample interacts with the standing wave formed in a Fabry–Perot cavity.[70] (b) Coherent counterpropagating waves of the same linear polarization form a standing wave of alternating electric and magnetic field antinodes that are sensitive to different multipole resonances.[72] (c) The electric dipole resonance of a plasmonic slot aperture metamaterial can be detected at the electric field antinode, but not at the magnetic field antinode (E node).[73] (d) The magnetic dipole and electric quadrupole resonance of stacked plasmonic wires can be detected at the magnetic field antinode, but not at the electric field antinode (B node).[73]

Instead, optical activity may be observed if the mirror-symmetry of the experimental arrangement is broken by the illumination direction. Such so-called "extrinsic 3D chirality" leads to very large optical activity in planar metamaterials lacking rotational symmetry[63] and this effect can also be coherently controlled. Coherent interaction of microwaves on an array of asymmetrically split metallic rings has allowed almost complete control over the ellipticity of electromagnetic waves from right-handed to left-handed circular polarization.[64] Figure 6b illustrates the first demonstration of such polarization control in the visible part of the spectrum.[65] Constructive (or destructive) interference at oblique incidence is achieved by illuminating both sides of the metamaterial with coherent waves incident in the same plane with the same incidence angle on the same side of the surface normal as shown. This way, the phase difference between the incident waves is constant across the metamaterial. The metamaterial is an asymmetric split ring aperture array in a gold film with ~300 nm period. Oblique incidence yields an extrinsically chiral experimental arrangement (except when the structure's line of symmetry coincides with the plane of incidence). The manifestation of the resulting optical activity is then controlled by the phase difference of the incident waves. For constructive interference of the incident electric fields significant circular dichroism (as well as circular birefringence) is observed, which increases with increasing angle of incidence. In contrast, destructive interference renders the nanostructure essentially transparent causing all polarization effects to vanish.

Coherent interaction of light-with-light on thin films can also be exploited to control light emission. For example, Pirruccio et al. reported that photoluminescence may be enhanced or suppressed through interference of pump light on a luminescent thin film[68] or on plasmonic nanostructures coupled to a luminescent material[66] (Figure 6c), providing a route to phase-modulated light sources.

Not only linear, but also nonlinear phenomena can be controlled by two coherent beams of light. This has been explored by Rao et al.[67] who studied nonlinear four-wave mixing in 30-layer graphene, which is about 9 nm thick, at a wavelength of 780 nm. By controlling the interference of two counterpropagating coherent pump beams on the thin graphene film (or one pump beam and its reflection on a mirror), the authors were able to control phase conjugation in the graphene film, see Figure 6d.

Coherent Excitation-Selective Spectroscopy. Important differences between interactions of light and matter in traveling and standing waves have previously been noted in the context of cavity ringdown spectroscopy[69,70] (Figure 7a), where different levels of absorption were observed for thin samples positioned at a node or antinode of a standing wave formed within a cavity. Standing waves, formed by counter-propagating coherent waves, offer degrees of freedom that allow probing of materials of substantially subwavelength thickness in ways that are not possible with traveling waves. For example, non-radiating anapoles, formed by destructive interference of electric and toroidal dipoles, can be excited in this way.[71]

In particular, copolarized, counter-propagating, coherent linearly polarized waves form a standing wave of alternating electric and magnetic field nodes and antinodes, see Figure 7b. As electric field antinodes correspond to magnetic field nodes, and vice versa, this allows selective material excitation with electric or magnetic field only. This enables the selective detection of even parity multipole resonances (e.g., electric

DOI: 10.1021/acsphotonics.7b00921
ACS Photonics XXXX, XXX, XXX−XXX

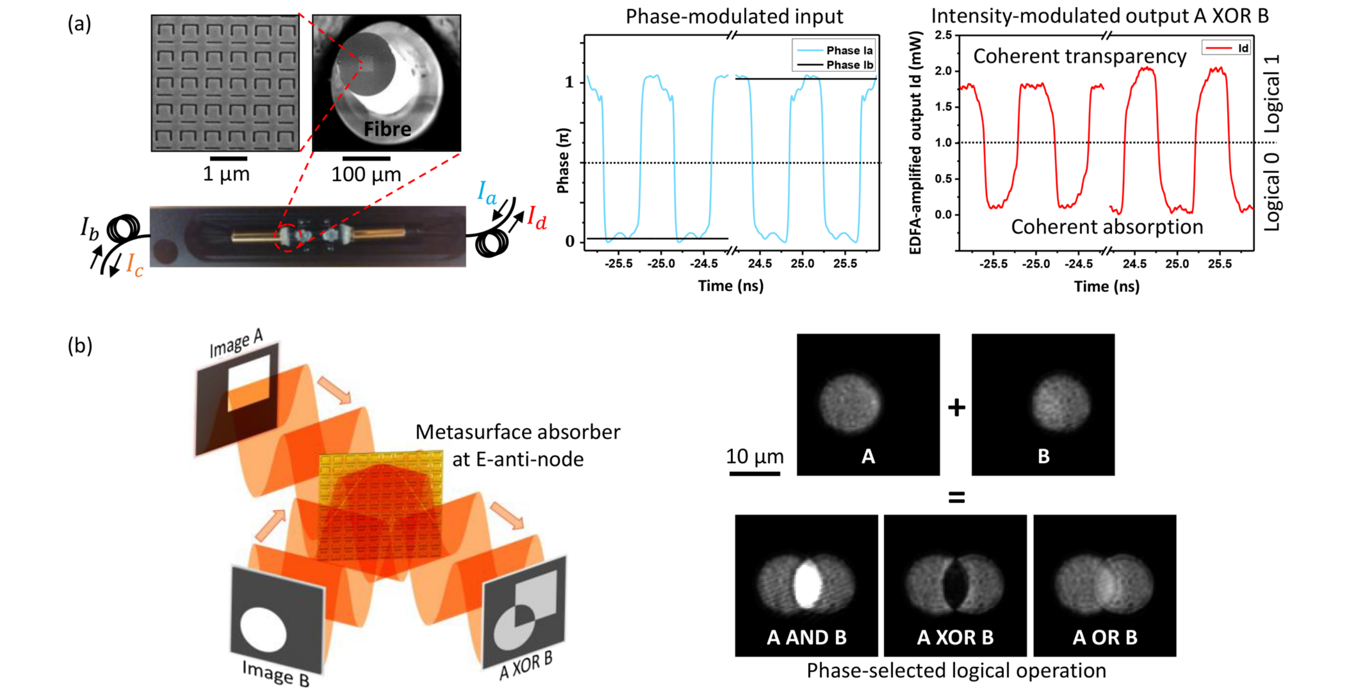

Figure 8. Coherent data and image processing. (a) Fiberized coherent data processing metadevice consisting of a gold metasurface absorber fabricated on the cleaved end of an optical fiber. Phase-modulated input signals I_a and I_b interact on the metasurface such that identical bits are absorbed and opposite bits are transmitted, yielding an output signal I_d corresponding to an intensity-modulated signal A XOR B with a modulation rate of 1.2 GHz.[76] (b) Logical operations between images, A and B, based on projection of both images onto a metasurface absorber using coherent light. The optical phase difference in areas of image overlap controls absorption from coherent perfect transparency to coherent perfect absorption and may be set to realize logical operations A AND B, A XOR B, and A OR B between the images.[77]

dipole) of a thin sample placed at an electric field antinode and detection of odd parity multipole resonances (e.g., magnetic dipole and electric quadrupole) at magnetic field antinodes.[72] Such excitation-selective spectroscopy in standing waves has been demonstrated experimentally by Fang et al.[73] using thin plasmonic metamaterials. The electric dipole resonance of an array of slots in a single plasmonic metal layer was clearly visible for electric field excitation but could not be detected with magnetic excitation (Figure 7c). In contrast, the magnetic dipole and electric quadrupole resonance of plasmonic wire pairs could only be detected with magnetic excitation of the nanostructure (Figure 7d).

Standing waves formed by copolarized, counterpropagating waves are only one type within a much bigger family of electromagnetic energy and polarization standing waves[74] promising further spectroscopic opportunities. Energy standing waves can be formed by counterpropagating coherent waves of parallel linear polarization or opposite circular polarizations and they are characterized by spatially oscillating electric and magnetic energy densities. Polarization standing waves are formed by counterpropagating waves of orthogonal linear polarization or identical circular polarization and they are characterized by a spatially oscillating local polarization state. As Fang et al.[74] have shown recently, they offer an additional degree of freedom for spectroscopy and control of light-matter interactions dependent on planar structural symmetries.

Data and Image Processing with Coherent Metadevices. The signal processing opportunities presented by coherent interaction of light-with-light on 2D matter in a four-port device, as discussed above, have been investigated in detail in a theoretical study by Fang et al.,[75] followed by recent experimental demonstrations.[76−78] They include transistor-like small-signal amplification as well as logical operations NOT, XOR, XNOR on phase-modulated data and NOT, XOR, AND, OR on intensity-modulated data, promising fast and low energy information processing in the locally coherent networks that are becoming part of the mainstream telecommunications agenda. With 100 THz bandwidth[47] and energy requirements at the quantum level[48] (see next section), coherent control of light-with-light on 2D matter may therefore provide part of the answer to the bandwidth and energy challenges in optical telecommunications.

Recently, a first fiberized coherent data processing system has been demonstrated,[76] see Figure 8a. It consists of a plasmonic metasurface absorber fabricated on the core area of a cleaved optical fiber coupled to a second optical fiber by a pair of microcollimator lenses. The fully packaged four-port metadevice connects directly to standard telecoms fibers. It exhibits the effective nonlinearity introduced in Figure 3 as well as several logical functions. For example, an XOR operation on binary phase-modulated data, where logical states of "1" and "0" are represented by equal intensity and opposite phase, is shown by Figure 8a. The XOR operation between input signals A and B results from absorption of identical bits due to constructive interference on the metasurface absorber and transmission of opposite bits due to destructive interference on the metasurface, yielding an intensity-modulated output signal A XOR B that has been demonstrated at modulation frequencies of up to 1.2 GHz. Other signal processing functions such as signal inversion have been demonstrated at effective bitrates of up to 40 Gbit/s.

In contrast to electronics, where every signal requires a separate wire, massively parallel information processing is easily realized in optics, where imaging systems transmit essentially

DOI: 10.1021/acsphotonics.7b00921
ACS Photonics XXXX, XXX, XXX−XXX

separate information channels spaced by the diffraction limit. Therefore, "zero-dimensional" coherent control of one beam of light with another, as considered above, may be extended to "two-dimensional" coherent control of light with light by projecting different images onto opposite sides of a metasurface absorber using coherent light, see Figure 8b. This has been demonstrated by Papaioannou et al.[77] for the simple case of imaging two misaligned apertures onto a metasurface absorber. In the regions of image overlap, the phase difference between the illuminating light beams controls absorption of light by the metasurface. Destructive interference in areas of image overlap highlights the similarities of images A and B due to coherent perfect transparency and therefore yields an output image A AND B. On the other hand, constructive interference deletes the similarities by coherent absorption, leaving only the image differences and therefore yields an output image A XOR B. The phase-dependent power variation of the output image is therefore proportional to the area of image overlap, while the minimum power contained in the output image is a measure of the image differences, enabling pattern recognition and image analysis applications.[79] Further importance is derived from the exponential growth of telecommunications bandwidth that will require information transfer in multiple spatial information channels, for example, in multicore optical fibers. Here, two-dimensional control of light with light can provide solutions for both ultrafast parallel data processing as well as selection and deletion of selected information channels.[78]

However, despite demonstrations of various single-channel and multichannel signal processing operations, there are still significant challenges that need to be overcome before complex coherent information processing systems can become a reality,[80] for example relating to phase stability and cascading of multiple signal processing steps. The phase stability that will be required across the entire system may be achieved by miniaturization and a monolithic platform that could be based on silicon photonics. Cascading of coherent signal processing steps will require the output of one coherent interaction to be a suitable input for the next, implying that signal regeneration may be needed in between signal processing steps to avoid accumulation of noise.

Coherent Absorption of Light in the Quantum Regime. Conventional modulation of light-with-light based on optical nonlinearities is strongly intensity-dependent and requires a minimum level of intensity to activate the nonlinear response. In contrast, coherent control of light-with-light as discussed above is linear in the sense that equal scaling of all coherent signals incident on a 2D material will result in scaling of all output signals by the same factor. Recently, it has been demonstrated that this remains true at arbitrarily low intensities and even in the single photon regime,[48] unlocking interesting and counterintuitive opportunities for deterministic control of single as well as entangled quanta of light.

Historically, losses and dissipation have typically been considered highly undesirable in the field of quantum optics[81] as losses occur at the expense of additional fluctuations and noise in the system.[82,83] It was therefore generally thought that dissipation should at all costs be minimized or avoided. However, recent advances in the field of quantum plasmonics[84] have paved the way to the study of quantum effects in the context of coherent perfect absorption. While absorption of photons from a traveling wave is probabilistic, coherent perfect absorption can be observed deterministically even with a single photon, which may be coupled into a localized plasmon with nearly 100% probability.[48] Also, two-photon N00N states can be commanded to exclusively exhibit either single- or two-photon absorption.[85] A counterintuitive and currently debated possibility is that dissipation can actually lengthen the coherence time of a certain subsystem thus possibly even providing a route for the observation of quantum effects in "warm" environments such as photosynthesis or other biological systems.[86−88]

More specifically to the control of photon states, the presence of loss, if properly harnessed, can be used as a resource that can shape the specific output modes from a beamsplitter in ways that are not achievable without loss. The first theoretical studies in this sense were carried out by Barnett and co-workers who analyzed the behavior of a lossy beamsplitter inserted in a Hong-Ou-Mandel interferometer.[89]

Hong-Ou-Mandel interference is a quantum effect whereby two photons simultaneously entering two ports of a beam splitter will be forced to bunch together, that is, they can exit from either output port, but both photons must exit from the same port.[90] It is not possible to know which output port the two photons will bunch into. Therefore, two photons interfering at the beamsplitter will create what is known as a N00N state at the beamsplitter output. A N00N state is an entangled state and is so-called after the bra-ket notation used to describe the situation in which 2 photons (or N photons) are in a superposition state of being either N in one arm or N in the other arm of an interferometer. Such path-entangled states can be used as a resource for quantum metrology as they can provide an N-fold enhancement in interferometer-based phase measurements. N00N states from photon bunching at a beamsplitter are generally obtained with a lossless beamsplitter. The more general case in which loss occurs at the beamsplitter leads to more complicated output states. Without going into the details of the most general case studied by Barnett et al.,[89] we will consider the specific situation in which absorption is equal to exactly 50% in a very thin film (compared to the wavelength of the photon). For the simplest case of a single photon input state ($N = 1$) with appropriate phases, the single photon is either deterministically absorbed or completely transmitted, thus, providing a "lossless lossy beamsplitter".[91] This of course is just a quantum restatement of coherent perfect absorption for a single photon.[92] Coherent perfect absorption of a single photon was verified experimentally by Roger et al., thereby extending coherent perfect absorption into the single photon regime.[48] For appropriate two-photon input states ($N = 2$), the lossy beam splitter can yield deterministic absorption of a single photon as well as situations where the two photons must be either both transmitted or both absorbed. The latter is reminiscent of nonlinear absorption processes although it is important to recall that the "linear" two-photon absorption described here requires linear absorption at the input wavelength of the two input photons (in contrast to nonlinear two-photon absorption that can occur in a medium that is transparent at the input wavelength). Thus, quantum states in the regime of coherent perfect absorption can lead to rather unexpected output states and situations such as linear two-photon absorption that do not have a direct analogue in classical optics. The first experimental verification of coherent perfect absorption with two-photon N00N states was performed by Roger et al. and was carried out using a multilayer graphene beamsplitter.[85] By tailoring the number of layers (2.3% absorption per layer), it is possible to achieve close to ideal 50% absorption in a graphene film of several nm

DOI: 10.1021/acsphotonics.7b00921
ACS Photonics XXXX, XXX, XXX−XXX

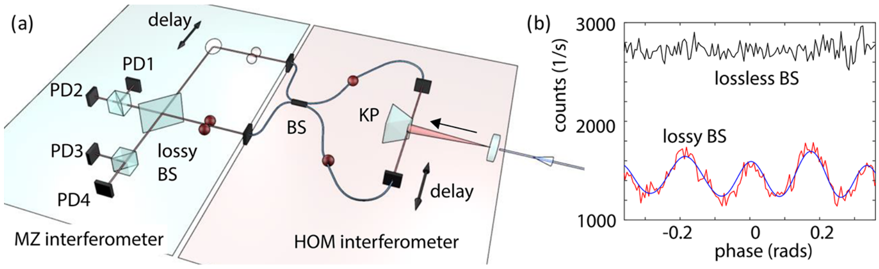

Figure 9. Coherent absorption in the quantum regime. (a) Experimental layout used to measure coherent perfect absorption with entangled N00N states. Photon pairs generated in a BBO crystal are filtered and split at a knife edge prism (KP). They are then coupled into the Hong-Ou-Mandel interferometer with single mode fibers and directed to a 50/50 beamsplitter (BS). A delay stage ensures the photons arrive at the same time on the beamsplitter and hence bunch, forming a N00N state. The $N = 2$ N00N state is directed into a Sagnac or, in this case, a Mach−Zehnder (MZ) interferometer. The N00N state interferes with itself on the lossy beam splitter and the output states are characterized by a series of four photon detectors (PD) and beamsplitters. (b) By scanning the N00N state phase with a delay stage, oscillations are seen in the total output coincidence counts. These correspond to the output state oscillating between a mixed state and a pure entangled N00N state with one photon less ($N = 1$). The black line shows the same measurement performed with a lossless beamsplitter: no oscillations in the coincidence counts are observed, reflecting the fact that the photon number is conserved.

thickness deposited on a glass substrate that is then used as the lossy beamsplitter. The input states are generated in a Hong-Ou-Mandel interferometer that is, in turn, illuminated with photon pairs obtained by parametric down-conversion in a BBO crystal. The output of the Hong-Ou-Mandel interferometer is fed into a Sagnac-interferometer, similar to that used for classical coherent perfect absorption measurements. The output states are then measured by extracting 50% of the photons with beamsplitters placed on either side of the lossy film. In this way it was indeed possible to verify that by changing the phase of the input states, the total photon counts oscillate, thus providing indirect evidence of the oscillation between single and two-photon absorption.

The extra degree of freedom offered by loss can also be used to achieve other forms of coherent control of quantum states. For example, Vest et al, showed that loss can lead to antibunching of bosons in a Hong-Ou-Mandel interferometer,[93] that is, the Hong-Ou-Mandel interferometer "dip" is replaced by a "peak". This Fermionic anticoalescence of photons at a beamsplitter, here obtained as a result of dissipation at the beamsplitter, had only been observed before by purposely shaping the input photons so that their wave functions where antisymmetric. Here, the common notion of boson bunching on a dielectric beamsplitter is overturned by resorting to the unique degree of freedom offered by lossy beamsplitters in tailoring the exact phase relation between reflection and transmission.

As a last example of progress in the field, we highlight recent work that extends previous quantum eraser experiments to include coherent perfect absorption.[94] If we consider the simple case of single photon interference, this may be inhibited by providing which-path information in the interferometer (e.g., by polarization rotation with a wave plate in one arm). During the postmeasurement process, it is however possible to "erase" the information by postselecting data based on measurements performed on a nonlocal detector.[95,96] The erasure scheme is enabled by entanglement of the photon inside the interferometer and the "control" photon, detected outside (nonlocally to) the interferometer. In the experiment by Altuzarra et al., a single photon is sent into a coherent perfect absorption interferometer such as that shown in Figure 9. The photon is one of a pair of polarization entangled photons; for example, the polarization of an individual photon is either vertical or horizontal but is not predetermined in a single measurement. However, measurement of the polarization of one photon fixes the polarization of the other to be opposite. Which-path information is introduced by a half-wave plate oriented at 45° inside only one arm of the interferometer: H-polarized photons traveling in that arm will be rotated to V and vice versa. Therefore, measurements performed on the single photon in the interferometer do not reveal any coherent perfect absorption effects due to the fact that the counterpropagating photon mode functions are oppositely polarized and can no longer form an energy standing wave. However, polarization sensitive measurements on the second (nonlocal) photon allow to immediately establish the polarization of the other photon: by postselecting all measurements corresponding to a fixed polarization of ±45° at the nonlocal detector, one fixes the polarization to ∓45° in the interferometer (that is not modified by the half-wave plate): which-path information is erased and coherent perfect absorption interference fringes are now observed. The quantum nature of this process is also directly verified by reducing the degree of entanglement of the two input photons and thus observing a corresponding decrease in the coherent perfect absorption visibility.[94]

This brief overview of recent results shows how absorption is gaining recognition as a resource in quantum optics and as such, coherent control of absorption presents new opportunities for both fundamental studies and applications alike, enriching the quantum toolbox.

■ SUMMARY

Control of light-with-light used to be the domain of nonlinear optics, however, the coherent interaction of light-with-light on linear dispersive planar materials and metamaterials enables control over a huge range of optical phenomena. Instead of relying on optically nonlinear materials, dynamic control of light-with-light is derived from the fact that the interference of two coherent beams of light controls the local field that interacts with the film. This allows the manifestation of the film's optical functionalities to be controlled from complete suppression by destructive interference to enhancement by constructive interference. In contrast to optical nonlinearities, such coherent control of light-with-light offers high contrast and high bandwidth and works at arbitrary intensities down to the single photon regime. Therefore, this approach offers a broad range of novel and interesting opportunities for classical all-optical signal and image processing as well as quantum

DOI: 10.1021/acsphotonics.7b00921
ACS Photonics XXXX, XXX, XXX−XXX

technologies. In addition, interference of coherent light fields allows selective probing of thin films with either electric or magnetic fields, opening up novel opportunities for spectroscopy.

AUTHOR INFORMATION

Corresponding Authors

*E-mail: erp@orc.soton.ac.uk.
*E-mail: kfm@orc.soton.ac.uk.
*E-mail: niz@orc.soton.ac.uk.

ORCID

Eric Plum: 0000-0002-1552-1840

Notes

The authors declare no competing financial interest.

ACKNOWLEDGMENTS

The authors thank Jianfa Zhang, Maria Papaioannou, Angelos Xomalis, Yidong Chong, and Robert Boyd for fruitful discussions. This work is supported by the U.K.'s Engineering and Physical Sciences Research Council (Grant EP/M009122/1) and the MOE Singapore (Grant MOE2011-T3-1-005). No new data were created as part of this review.

REFERENCES

(1) Shapiro M, B. P. *Principles of the Quantum Control of Molecular Processes*; John Wiley & Sons Inc.: New York, 2003.

(2) Reiter, D. E.; Sherman, E. Y.; Najmaie, A.; Sipe, J. E. Coherent control of electron propagation and capture in semiconductor heterostructures. *Europhys. Lett.* **2009**, *88* (6), 67005.

(3) Assion, A.; Baumert, T.; Bergt, M.; Brixner, T.; Kiefer, B.; Seyfried, V.; Strehle, M.; Gerber, G. Control of Chemical Reactions by Feedback-Optimized Phase-Shaped Femtosecond Laser Pulses. *Science* **1998**, *282* (5390), 919−922.

(4) Chong, Y. D.; Ge, L.; Cao, H.; Stone, A. D. Coherent Perfect Absorbers: Time-Reversed Lasers. *Phys. Rev. Lett.* **2010**, *105*, 053901.

(5) Wan, W.; Chong, Y.; Ge, L.; Noh, H.; Stone, A. D.; Cao, H. Time-Reversed Lasing and Interferometric Control of Absorption. *Science* **2011**, *331*, 889−892.

(6) Yoon, J. W.; Koh, G. M.; Song, S. H.; Magnusson, R. Measurement and Modeling of a Complete Optical Absorption and Scattering by Coherent Surface Plasmon-Polariton Excitation Using a Silver Thin-Film Grating. *Phys. Rev. Lett.* **2012**, *109*, 257402.

(7) Noh, H.; Chong, Y.; Stone, A. D.; Cao, H. Perfect coupling of light to surface plasmons by coherent absorption. *Phys. Rev. Lett.* **2012**, *108*, 186805.

(8) Pye, L. N.; Villinger, M. L.; Shabahang, S.; Larson, W. D.; Martin, L.; Abouraddy, A. F. Octave-spanning coherent perfect absorption in a thin silicon film. *Opt. Lett.* **2017**, *42* (1), 151−154.

(9) Stockman, M. I.; Faleev, S. V.; Bergman, D. J. Coherent Control of Femtosecond Energy Localization in Nanosystems. *Phys. Rev. Lett.* **2002**, *88*, 067402.

(10) Li, X.; Stockman, M. I. Highly efficient spatiotemporal coherent control in nanoplasmonics on a nanometer-femtosecond scale by time reversal. *Phys. Rev. B: Condens. Matter Mater. Phys.* **2008**, *77*, 195109.

(11) Kao, T. S.; Jenkins, S. D.; Ruostekoski, J.; Zheludev, N. I. Coherent Control of Nanoscale Light Localization in Metamaterial: Creating and Positioning Isolated Subwavelength Energy Hot Spots. *Phys. Rev. Lett.* **2011**, *106*, 085501.

(12) Gjonaj, B.; Aulbach, J.; Johnson, P. M.; Mosk, A. P.; Kuipers, L.; Lagendijk, A. Active spatial control of plasmonic fields. *Nat. Photonics* **2011**, *5*, 360−363.

(13) Brinks, D.; Castro-Lopez, M.; Hildner, R.; van Hulst, N. F. Plasmonic antennas as design elements for coherent ultrafast nanophotonics. *Proc. Natl. Acad. Sci. U. S. A.* **2013**, *110*, 18386−18390.

(14) Scalora, M.; Bloemer, M. J.; Pethel, A. S.; Dowling, J. P.; Bowden, C. M.; Manka, A. S. Transparent, metallo-dielectric, one-dimensional, photonic band-gap structures. *J. Appl. Phys.* **1998**, *83* (5), 2377−2383.

(15) Scalora, M.; Bloemer, M. J.; Bowden, C. M. Metals under a new light. *Opt. Photonics News* **1999**, *10* (9), 25−27.

(16) Bruck, R.; Muskens, O. L. Plasmonic nanoantennas as integrated coherent perfect absorbers on SOI waveguides for modulators and all-optical switches. *Opt. Express* **2013**, *21* (23), 27662−71.

(17) Park, H.; Lee, S. Y.; Kim, J.; Lee, B.; Kim, H. Near-infrared coherent perfect absorption in plasmonic metal-insulator-metal waveguide. *Opt. Express* **2015**, *23* (19), 24464−74.

(18) Rothenberg, J. M.; Chen, C. P.; Ackert, J. J.; Dadap, J. I.; Knights, A. P.; Bergman, K.; Osgood, R. M.; Grote, R. R. Experimental demonstration of coherent perfect absorption in a silicon photonic racetrack resonator. *Opt. Lett.* **2016**, *41* (11), 2537−40.

(19) Utikal, T.; Stockman, M. I.; Heberle, A. P.; Lippitz, M.; Giessen, H. All-Optical Control of the Ultrafast Dynamics of a Hybrid Plasmonic System. *Phys. Rev. Lett.* **2010**, *104*, 113903.

(20) Papoff, F.; McArthur, D.; Hourahine, B. Coherent control of radiation patterns of nonlinear multiphoton processes in nanoparticles. *Sci. Rep.* **2015**, *5*, 12040.

(21) Crescimanno, M.; Dawson, N. J.; Andrews, J. H. Coherent perfect rotation. *Phys. Rev. A: At., Mol., Opt. Phys.* **2012**, *86*, 031807.

(22) Crescimanno, M.; Zhou, C.; Andrews, J. H.; Baker, M. A. Structure and symmetry in coherent perfect polarization rotation. *Phys. Rev. A: At., Mol., Opt. Phys.* **2015**, *91* (1), 013845.

(23) Friedrich, D.; Kaufer, H.; Westphal, T.; Yamamoto, K.; Sawadsky, A.; Khalili, F. Y.; Danilishin, S. L.; Goßler, S.; Danzmann, K.; Schnabel, R. Laser interferometry with translucent and absorbing mechanical oscillators. *New J. Phys.* **2011**, *13*, 093017.

(24) Yan, X. B.; Cui, C. L.; Gu, K. H.; Tian, X. D.; Fu, C. B.; Wu, J. H. Coherent perfect absorption, transmission, and synthesis in a double-cavity optomechanical system. *Opt. Express* **2014**, *22* (5), 4886−4895.

(25) Choi, S. B.; Park, D. J.; Jeong, Y. K.; Yun, Y. C.; Jeong, M. S.; Byeon, C. C.; Kang, J. H.; Park, Q. H.; Kim, D. S. Directional control of surface plasmon polariton waves propagating through an asymmetric Bragg resonator. *Appl. Phys. Lett.* **2009**, *94*, 063115.

(26) Li, Z.; Zhang, S.; Halas, N. J.; Nordlander, P.; Xu, H. Coherent Modulation of Propagating Plasmons in Silver-Nanowire-Based Structures. *Small* **2011**, *7*, 593−596.

(27) Miyata, M.; Takahara, J. Excitation control of long-range surface plasmons by two incident beams. *Opt. Express* **2012**, *20*, 9493−9500.

(28) Wei, P.; Croënne, C.; Tak Chu, S.; Li, J. Symmetrical and anti-symmetrical coherent perfect absorption for acoustic waves. *Appl. Phys. Lett.* **2014**, *104* (12), 121902.

(29) Meng, C.; Zhang, X.; Tang, S. T.; Yang, M.; Yang, Z. Acoustic Coherent Perfect Absorbers as Sensitive Null Detectors. *Sci. Rep.* **2017**, *7*, 43574.

(30) Pozar, D. M. *Microwave Engineering*, 2nd ed.; John Wiley & Sons Inc., 1998.

(31) Jackson, J. D. *Classical Electrodynamics*, 3rd ed.; John Wiley & Sons: New York, 1998.

(32) Troitskii, Y. V. Optical resonator with a thin absorbing film as a mode selector. *Opt. Spectrosc.* **1968**, *25*, 309−313.

(33) Troitskii, Y. V.; Goldina, N. D. Separation of one mode in a laser. *JETP Lett.* **1968**, *7*, 36.

(34) Smith, P. W.; Schneider, M. V.; Danielmeyer, H. G. High-Power Single-Frequency Lasers Using Thin Metal Film Mode-Selection Filters. *Bell Syst. Tech. J.* **1969**, *48*, 1405.

(35) Avtonomov, V. P.; Antropov, E. T.; Sobolev, N. N.; Troitskii, Y. V. Separation of rotational lines of a CO2 laser with a film selector in the resonator. *Sov. J. Quantum Electron* **1972**, *2* (3), 300−302.

(36) Miller, A. B. Laser tuners and wavelength-selective detectors based on absorbers in standing waves. *IEEE J. Quantum Electron.* **1994**, *30* (3), 732−749.

(37) Babin, S. A.; Kablukov, S. I.; Terentiev, V. S. Reflection interferometer based on the Troitsky thin film for frequency selection in fiber lasers. *Laser Phys.* **2008**, *18* (11), 1241−1245.

(38) Hägglund, C.; Apell, S. P.; Kasemo, B. Maximized Optical Absorption in Ultrathin Films and Its Application to Plasmon-Based Two-Dimensional Photovoltaics. *Nano Lett.* **2010**, *10*, 3135−3141.

(39) Thongrattanasiri, S.; Koppens, F. H. L.; García de Abajo, F. J. Complete Optical Absorption in Periodically Patterned Graphene. *Phys. Rev. Lett.* **2012**, *108*, 047401.

(40) Zhang, J.; MacDonald, K. F.; Zheludev, N. I. Controlling light-with-light without nonlinearity. *Light: Sci. Appl.* **2012**, *1*, e18.

(41) Dutta-Gupta, S.; Martin, O. J. F.; Dutta Gupta, S.; Agarwal, G. S. Controllable coherent perfect absorption in a composite film. *Opt. Express* **2012**, *20*, 1330−1336.

(42) Yu, S.; Piao, X.; Hong, J.; Park, N. Progress toward high-Qperfect absorption: A Fano antilaser. *Phys. Rev. A: At., Mol., Opt. Phys.* **2015**, *92* (1), 011802(R).

(43) Wong, Z. J.; Xu, Y.-L.; Kim, J.; O'Brien, K.; Wang, Y.; Feng, L.; Zhang, X. Lasing and anti-lasing in a single cavity. *Nat. Photonics* **2016**, *10* (12), 796−801.

(44) Zheludev, N. I.; Kivshar, Y. S. From metamaterials to metadevices. *Nat. Mater.* **2012**, *11*, 917−924.

(45) Plum, E.; Tanaka, K.; Chen, W. T.; Fedotov, V. A.; Tsai, D. P.; Zheludev, N. I. A combinatorial approach to metamaterials discovery. *J. Opt.* **2011**, *13*, 055102.

(46) Fang, X.; Tseng, M. L.; Ou, J. Y.; MacDonald, K. F.; Tsai, D. P.; Zheludev, N. I. Ultrafast all-optical switching via coherent modulation of metamaterial absorption. *Appl. Phys. Lett.* **2014**, *104*, 141102.

(47) Nalla, V.; Valente, J.; Sun, H.; Zheludev, N. I. 11-fs dark pluses generated via coherent absorption in plasmonic metamaterial. *Opt. Express* **2017**, *25* (19), 22620−22625.

(48) Roger, T.; Vezzoli, S.; Bolduc, E.; Valente, J.; Heitz, J. J. F.; Jeffers, J.; Soci, C.; Leach, J.; Couteau, C.; Zheludev, N. I.; Faccio, D. Coherent perfect absorption in deeply subwavelength films in the single-photon regime. *Nat. Commun.* **2015**, *6*, 7031.

(49) Nalla, V.; Karvounis, A.; Valente, J.; Sun, H. D.; Zheludev, N. I. Ultrafast Regimes of Coherent Absorption in Plasmonic and Dielectric Diamond-Based Metasurfaces. *ICMAT2017*, Singapore, 2017.

(50) Fan, Y.; Liu, Z.; Zhang, F.; Zhao, Q.; Wei, Z.; Fu, Q.; Li, J.; Gu, C.; Li, H. Tunable mid-infrared coherent perfect absorption in a graphene meta-surface. *Sci. Rep.* **2015**, *5*, 13956.

(51) Nie, G.; Shi, Q.; Zhu, Z.; Shi, J. Selective coherent perfect absorption in metamaterials. *Appl. Phys. Lett.* **2014**, *105*, 201909.

(52) Pu, M.; Feng, Q.; Wang, M.; Hu, C.; Huang, C.; Ma, X.; Zhao, Z.; Wang, C.; Luo, X. Ultrathin broadband nearly perfect absorber with symmetrical coherent illumination. *Opt. Express* **2012**, *20*, 2246−2254.

(53) Rao, S. M.; Heitz, J. J. F.; Roger, T.; Westerberg, N.; Faccio, D. Coherent control of light interaction with graphene. *Opt. Lett.* **2014**, *39* (18), 5345−5374.

(54) Boyd, R. W. *Nonlinear Opt.*, 3rd ed.; Academic Press: San Diego, CA, U.S.A., 2008.

(55) Shi, J.; Fang, X.; Rogers, E. T. F.; Plum, E.; MacDonald, K. F.; Zheludev, N. I. Coherent control of Snell's law at metasurfaces. *Opt. Express* **2014**, *22* (17), 21051−21060.

(56) Yu, N.; Genevet, P.; Kats, M. A.; Aieta, F.; Tetienne, J.-P.; Capasso, F.; Gaburro, Z. Light Propagation with Phase Discontinuities: Generalized Laws of Reflection and Refraction. *Science* **2011**, *334* (6054), 333−337.

(57) Kita, S.; Takata, K.; Ono, M.; Nozaki, K.; Kuramochi, E.; Takeda, K.; Notomi, M. Coherent control of high efficiency metasurface beam deflectors with a back partial reflector. *APL Photonics* **2017**, *2* (4), 046104.

(58) Ni, X.; Ishii, S.; Kildishev, A. V.; Shalaev, V. M. Ultra-thin, planar, Babinet-inverted plasmonic metalenses. *Light: Sci. Appl.* **2013**, *2* (4), e72.

(59) Chen, X.; Huang, L.; Muhlenbernd, H.; Li, G.; Bai, B.; Tan, Q.; Jin, G.; Qiu, C. W.; Zhang, S.; Zentgraf, T. Dual-polarity plasmonic metalens for visible light. *Nat. Commun.* **2012**, *3*, 1198.

(60) Ni, X.; Kildishev, A. V.; Shalaev, V. M. Metasurface holograms for visible light. *Nat. Commun.* **2013**, *4*, 2807.

(61) Huang, L.; Chen, X.; Mühlenbernd, H.; Zhang, H.; Chen, S.; Bai, B.; Tan, Q.; Jin, G.; Cheah, K.-W.; Qiu, C.-W.; Li, J.; Zentgraf, T.; Zhang, S. Three-dimensional optical holography using a plasmonic metasurface. *Nat. Commun.* **2013**, *4*, 2808.

(62) Mousavi, S. A.; Plum, E.; Shi, J.; Zheludev, N. I. Coherent control of birefringence and optical activity. *Appl. Phys. Lett.* **2014**, *105*, 011906.

(63) Plum, E.; Liu, X. X.; Fedotov, V. A.; Chen, Y.; Tsai, D. P.; Zheludev, N. I. Metamaterials: optical activity without chirality. *Phys. Rev. Lett.* **2009**, *102* (11), 113902.

(64) Mousavi, S. A.; Plum, E.; Shi, J.; Zheludev, N. I. Coherent control of optical polarization effects in metamaterials. *Sci. Rep.* **2015**, *5*, 8977.

(65) Hiramatsu, K.; Plum, E.; Valente, J.; MacDonald, K. F.; Zheludev, N. I. *Coherent Spectroscopy of Optical Activity*. *CLEO/Europe-EQEC 2015*, Munich, Germany, 21−25 June 2015; Munich, Germany, 2015.

(66) Pirruccio, G.; Ramezani, M.; Rodriguez, S. R.; Rivas, J. G. Coherent Control of the Optical Absorption in a Plasmonic Lattice Coupled to a Luminescent Layer. *Phys. Rev. Lett.* **2016**, *116* (10), 103002.

(67) Rao, S. M.; Lyons, A.; Roger, T.; Clerici, M.; Zheludev, N. I.; Faccio, D. Geometries for the coherent control of four-wave mixing in graphene multilayers. *Sci. Rep.* **2015**, *5*, 15399.

(68) Pirruccio, G.; Rivas, J. G. Modulated light absorption and emission of a luminescent layer by phase-controlled multiple beam illumination. *Opt. Express* **2015**, *23* (14), 18166−80.

(69) Terasaki, A.; Kondow, T.; Egashira, K. Continuous-wave cavity ringdown spectroscopy applied to solids: properties of a Fabry-Perot cavity containing a transparent substrate. *J. Opt. Soc. Am. B* **2005**, *22* (3), 675−686.

(70) Egashira, K.; Terasaki, A.; Kondow, T. Photon-trap spectroscopy applied to molecules adsorbed on a solid surface: probing with a standing wave versus a propagating wave. *Appl. Opt.* **2010**, *49* (7), 1151−1157.

(71) Wei, L.; Xi, Z.; Bhattacharya, N.; Urbach, H. P. Excitation of the radiationless anapole mode. *Optica* **2016**, *3* (8), 799.

(72) Tseng, M. L.; Fang, X.; Savinov, V.; Wu, P. C.; Ou, J. Y.; Zheludev, N. I.; Tsai, D. P. Coherent selection of invisible high-order electromagnetic excitations. *Sci. Rep.* **2017**, *7*, 44488.

(73) Fang, X.; Tseng, M. L.; Tsai, D. P.; Zheludev, N. I. Coherent Excitation-Selective Spectroscopy of Multipole Resonances. *Phys. Rev. Appl.* **2016**, *5*, 014010.

(74) Fang, X.; MacDonald, K. F.; Plum, E.; Zheludev, N. I. Coherent control of light-matter interactions in polarization standing waves. *Sci. Rep.* **2016**, *6*, 31141.

(75) Fang, X.; MacDonald, K. F.; Zheludev, N. I. Controlling light with light using coherent metadevices: all-optical transistor, summator and invertor. *Light: Sci. Appl.* **2015**, *4*, e292.

(76) Xomalis, A.; Demirtzioglou, I.; Plum, E.; Jung, Y.; Nalla, V.; Lacava, C.; MacDonald, K. F.; Petropoulos, P.; Richardson, D. J.; Zheludev, N. I. Fibre-optic metadevice for all-optical signal modulation based on coherent absorption. *arXiv1709.05357*, **2017**.

(77) Papaioannou, M.; Plum, E.; Valente, J.; Rogers, E. T. F.; Zheludev, N. I. Two-dimensional control of light with light on metasurfaces. *Light: Sci. Appl.* **2016**, *5*, e16070.

(78) Papaioannou, M.; Plum, E.; Valente, J.; Rogers, E. T. F.; Zheludev, N. I. All-optical multichannel logic based on coherent perfect absorption in a plasmonic metamaterial. *APL Photonics* **2016**, *1*, 090801.

(79) Papaioannou, M.; Plum, E.; Zheludev, N. I. All-Optical Pattern Recognition and Image Processing on a Metamaterial Beam Splitter. *ACS Photonics* **2017**, *4* (2), 217−222.

(80) Miller, D. A. B. Are optical transistors the logical next step? *Nat. Photonics* **2010**, *4* (1), 3−5.

(81) Walls, D. F.; Milburn, G. J. Effect of dissipation on quantum coherence. *Phys. Rev. A: At., Mol., Opt. Phys.* **1985**, *31* (4), 2403−2408.

(82) Callen, H. B.; Welton, T. A. Irreversibility and Generalized Noise. *Phys. Rev.* **1951**, *83* (1), 34−40.

DOI: 10.1021/acsphotonics.7b00921
ACS Photonics XXXX, XXX, XXX−XXX

(83) Kubo, R. The fluctuation-dissipation theorem. *Rep. Prog. Phys.* **1966**, *29*, 255.
(84) Tame, M. S.; McEnery, K. R.; Özdemir, Ş. K.; Lee, J.; Maier, S. A.; Kim, M. S. Quantum plasmonics. *Nat. Phys.* **2013**, *9* (6), 329−340.
(85) Roger, T.; Restuccia, S.; Lyons, A.; Giovannini, D.; Romero, J.; Jeffers, J.; Padgett, M.; Faccio, D. Coherent Absorption of N00N States. *Phys. Rev. Lett.* **2016**, *117*, 023601.
(86) Müller, M.; Diehl, S.; Pupillo, G.; Zoller, P. Engineered Open Systems and Quantum Simulations with Atoms and Ions. *Adv. At., Mol., Opt. Phys.* **2012**, *61*, 1−80.
(87) Verstraete, F.; Wolf, M. M.; Ignacio Cirac, J. Quantum computation and quantum-state engineering driven by dissipation. *Nat. Phys.* **2009**, *5* (9), 633−636.
(88) Barreiro, J. T.; Muller, M.; Schindler, P.; Nigg, D.; Monz, T.; Chwalla, M.; Hennrich, M.; Roos, C. F.; Zoller, P.; Blatt, R. An open-system quantum simulator with trapped ions. *Nature* **2011**, *470* (7335), 486−491.
(89) Barnett, S.; Jeffers, J.; Gatti, A.; Loudon, R. Quantum optics of lossy beam splitters. *Phys. Rev. A: At., Mol., Opt. Phys.* **1998**, *57*, 2134−2145.
(90) Hong, C. K.; Ou, Z. Y.; Mandel, L. Measurement of Subpicosecond Time Intervals between Two Photons by Interference. *Phys. Rev. Lett.* **1987**, *59* (18), 2044−2046.
(91) Jeffers, J. Interference and the lossless lossy beam splitter. *J. Mod. Opt.* **2000**, *47*, 10.
(92) Huang, S.; Agarwal, G. S. Coherent perfect absorption of path entangled single photons. *Opt. Express* **2014**, *22* (17), 20936.
(93) Vest, B.; Dheur, M.-C.; Devaux, É.; Baron, A.; Rousseau, E.; Hugonin, J.-P.; Greffet, J.-J.; Messin, G.; Marquier, F. Anti-coalescence of bosons on a lossy beam splitter. *Science* **2017**, *356*, 1373.
(94) Altuzarra, C. M. X.; Vezzoli, S.; Valente, J.; Gao, W.; Soci, C.; Faccio, D.; Couteau, C. Coherent perfect absorption in metamaterials with entangled photons. *ACS Photonics* **2017**, *4*, 2124.
(95) Scully, M. O.; Drühl, K. Quantum eraser: A proposed photon correlation experiment concerning observation and ″delayed choice″ in quantum mechanics. *Phys. Rev. A: At., Mol., Opt. Phys.* **1982**, *25* (4), 2208−2213.
(96) Walborn, S. P.; Terra Cunha, M. O.; Pádua, S.; Monken, C. H. Double-slit quantum eraser. *Phys. Rev. A: At., Mol., Opt. Phys.* **2002**, *65* (3), 033818.

DOI: 10.1021/acsphotonics.7b00921
ACS Photonics XXXX, XXX, XXX−XXX